

Susceptibility and Knight-shift anomalies in cuprate superconductors

J. Thoma, S. Tewari, and J. Ruvalds

Physics Department, University of Virginia, Charlottesville, Virginia 22903

C. T. Rieck

Abteilung für Theoretische Festkörperphysik, Universität Hamburg, Hamburg, Germany

(Received 19 August 1994; revised manuscript received 27 December 1994)

The unconventional temperature variation of the static susceptibility $\chi(T)$ that has been discovered in various copper oxide superconductors is explained in terms of a model density of states that has a step shape at an energy threshold E_0 along with a logarithmic Van Hove singularity at the same E_0 . Calculations of $\chi(T)$ and the Knight shift above the superconducting transition temperature T_c yield good fits to the YBCO, BSCCO, and LSCO data by adjusting only the Fermi energy μ in correspondence to the oxygen or Sr content, respectively. When μ is right on or slightly below the Van Hove singularity, an upturn in χ occurs as the temperature T is lowered. By contrast, when μ is slightly above the threshold energy E_0 , a downturn in χ is achieved as T is lowered. A correlation of these phenomena with experimental data provides insight into the proximity of the Van Hove singularity to μ in several cuprate superconductors. The YBCO and TBCO cuprates with the higher T_c values exhibit a nearly constant susceptibility that suggests a Fermi energy well removed from the Van Hove singularity. The sensitivity of T_c as well as the susceptibility to chemical changes may provide tests of electronic mechanisms of electron pairing as well as the BCS theory.

I. BACKGROUND

Most ordinary metals exhibit the standard Pauli spin susceptibility $\chi(T)$ which is relatively independent of temperature T . The derivation of this result assumes a density of states whose energy variation is smooth on a scale comparable to T .

Magnetic measurements¹⁻⁸ on copper oxide alloys have revealed surprising temperature variations of χ in the metallic phases. These phenomena may have a bearing on the mechanism responsible for very high-superconducting transition temperatures T_c in certain compositions of these materials. Some of the cuprate alloys^{5,6} exhibit a nearly T -independent susceptibility above T_c , and the magnitude of χ corresponds to a conventional metallic density of states. However, an anomalous decrease in χ as T is lowered toward the superconducting transition has been observed¹⁻⁷ in numerous cuprates at selected oxygen compositions. This unexplained behavior provides the primary motivation for the present work.

Friedel⁹ has conjectured that a "pseudogap" structure in the density of states may be relevant to the susceptibility downturn at low T , but so far there has been no theoretical basis or development that is available for a quantitative analysis of the cuprate data. Furthermore, examples of an upturn in the susceptibility at low T have also been discovered^{3,8} in certain compositions of cuprates that display metallic transport properties, and such cases present yet another theoretical challenge.

The goal of the present study is to explain a wide range of anomalous susceptibility variations seen in cuprates in terms of a simple model of the electronic density of states. Our model contains a step shape at an energy threshold E_0 along with a logarithmic Van Hove singularity at the same E_0 . Such a model is reminiscent of the density of states produced by two-dimensional tight-binding energy bands if there is a narrow energy band whose maximum is very close to the Fermi energy. We shall demonstrate surprisingly good fits to the YBCO, LSCO, and BSCCO cuprate data using a model parameter set and adjusting only the chemical potential μ within a given cuprate family. The model should be relevant to other phenomena that are sensitive to the density of states, such as the heat capacity. On the other hand, transport properties and other features dominated by the shape of the Fermi surface are beyond the scope of the present work.

Band-structure calculations reveal narrow bands in cuprates that lie close to the Fermi energy as discussed in the review by Pickett.¹⁰ In the YBCO case, the band calculations of Mazin *et al.*¹¹ show a narrow band crossing that is particularly reminiscent of our model. Furthermore, the step structure in the density of states is supported by recent photoemission spectroscopy data on cuprates.¹²⁻¹⁵ The Fermi energy is found to be extremely close to a Van Hove singular peak in the density of states in the Bi2201 cuprate,¹⁶ and our work would predict an upturn in $\chi(T)$ at low T in that case. Recent photoemission data¹⁷ on $\text{YBa}_2\text{Cu}_4\text{O}_8$ provides Van Hove structural information, and the occurrence of a flat energy band near the Fermi energy seems to have been verified in $\text{Tl}_2\text{Ba}_2\text{CuO}_6$ as well.¹⁷ In the event that the Fermi energy intersects two bands, with one being almost filled, the susceptibility may also provide clues to electronic pairing mechanisms that require exciton or acoustic plasmon modes.

Although we defer the study of the susceptibility in the superconducting state to a later date, our present analysis

of the normal state reveals insight into the proximity of the Fermi energy to the Van Hove singularity. This has been cited by several groups as a possible key to high- T_c superconductivity, as discussed below.

An empirical connection between superconductivity and anomalous susceptibility variations in A -15 compounds was noticed more than 30 years ago.¹⁸ Alloys such as V_3Si and Nb_3Sn with $T_c = 18$ K exhibit a strong upturn in $\chi(T)$ at low temperatures, while some other A -15's with lower T_c values show a more conventional Pauli susceptibility with negligible T variation. On the other hand, compounds like Nb_3Ge and Nb_3Al display a standard Pauli behavior despite their high- T_c values. Clogston and Jaccarino¹⁹ attributed the susceptibility rise in A -15 compounds to a narrow peak in the density of states near the Fermi energy, whose width must be comparable to room temperature. A possible enhancement of the superconducting pairing by a quasi-one-dimensional Van Hove structure in the density of states was originally proposed by Labbé and Friedel²⁰ on the basis of a BCS mechanism of phonon exchange.

Logarithmic Van Hove singularities in the density of states are expected for a tight-binding band in two dimensions. The planar electronic structure of cuprates may lead to such sharp singularities, and this possibility may lead to enhanced phonon-mediated pairing of electrons as shown by Hirsch and Scalapino²¹ and Dzyaloshinski.²² More recent theories have claimed a link between Van Hove singularities and the abnormal transport properties of the cuprates. For example, Lee and Read²³ suggested that the unusual linear temperature variation of the resistivity that is a trademark of high- T_c cuprate superconductors could be caused by electron-electron scattering on a square (i.e., perfectly nested) Fermi surface that situates the chemical potential μ precisely at the Van Hove singularity. Newns *et al.*²⁴ and Markiewicz²⁵ have argued that similar logarithmic structures in the density of states provide the connection between the resistivity anomalies and the high-superconducting transition temperatures of cuprates. On the other hand, Radtke *et al.*²⁶ have published calculations that include strong-coupling effects and have concluded that logarithmic Van Hove peaks do not yield a significant increase in T_c .

We consider a logarithmic singularity in the density of states in order to shed light on the role of such structure in the static susceptibility. Comparisons of our calculated susceptibility to experimental data for the Knight shift in particular will establish guidelines for the proximity of the chemical potential to the Van Hove singularity, and thus provide constructive limits on theoretical proposals.

An interesting possible origin of the flat quasiparticle dispersion has been found in Monte Carlo calculations for the t - J model by Dagotto *et al.*²⁷ The existence of localized spins in insulating cuprates is described quite well by a two-dimensional antiferromagnetic Heisenberg model. Accordingly it is interesting that high- and low-temperature expansions of the Heisenberg model give rise to unusual temperature variations of the susceptibility.²⁸ Quantum Monte Carlo computations²⁹ for the t - J model yield a susceptibility whose temperature variation scale is set by the exchange coupling J . If $J \sim 1500$ K, as in the

insulating cuprates, the computed χ is hard to reconcile with the experiments on metallic cuprates that are considered in our work. However, an alternate explanation of the susceptibility anomalies²⁹ may be that the effective coupling J could be significantly reduced by doping. Thus it would be worthwhile to examine the rich experimental data in quantitative detail by these approaches as well.

Insulating cuprates are outside the scope of our analysis. Their antiferromagnetic order yields a characteristic shape in $\chi(T)$ below the Néel temperature that is quite different from the features found in the metallic cuprates discussed in the present work.

A remarkable correlation of measured T_c values with the metallic resistivity exponent n determined from its low-temperature behavior T^n is shown in Fig. 1 for various superconductors. The resistivity is linear in T for all of the optimally doped copper oxide compounds which have the highest transition temperatures. The power-law exponent in the cuprates changes as a function of doping (see, for example, Takagi *et al.*³⁰). Nested Fermi-surface segments are predicted to yield a linear T resistivity,³¹ while rounded corners should give the traditional T^2 behavior from electron collisions. Doping cuprates should generate a crossover from the linear T to a T^2 behavior, and this has been found for $Tl_2Ba_2CuO_{6+\delta}$.³⁰ By contrast, the conventional T^5 behavior due to phonon scattering is well known in Pb and Nb. It is interesting that the T^2 variation reminiscent of Fermi-liquid electron-electron scattering occurs in Ce-doped cuprates

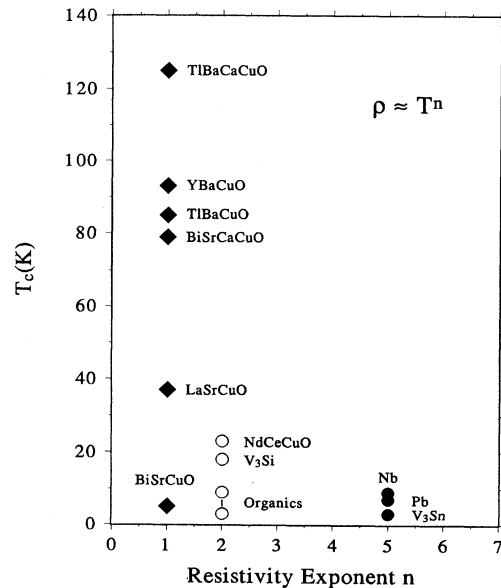


FIG. 1. The transition temperature of various superconductors is plotted vs the low-temperature power-law exponent n of the normal-state resistivity $\rho = T^n$. Conventional metals such as Pb and Nb which are BCS superconductors have a T^5 dependence, while the Ce-doped cuprates show a Fermi-liquid T^2 behavior. All of the higher T_c superconductors display a linear temperature variation of the resistivity.

and also in various organic metals. Evidently there is a compelling link between the mechanism responsible for the linear resistivity and high- T_c superconductivity.

A microscopic theory of the linear T variation of the resistivity has been developed on the basis of nesting of the Fermi surface in the form of nearly parallel orbit segments.³¹ Analytic derivations of the dynamic spin susceptibility $\chi''(\mathbf{Q}, \omega, T)$ predict a surprising scaling as a function of frequency ω divided by temperature T , where \mathbf{Q} is the nesting vector.³¹ This scaling behavior generates a linear T variation of the damping caused by electron-electron collisions, and evidence for the scaling phenomena³² has been seen in neutron-scattering measurements on YBCO.^{33,34} The neutron measurements require large single-crystal samples and only limited doping regimes have thus far been successfully tested. Nesting may occur in a tight-binding band even though the chemical potential is away from a Van Hove singularity. The real part of the static susceptibility at $\mathbf{q}=0$ can then be relatively independent of temperature even though the dynamic scaling in $\chi''(\mathbf{Q}, \omega/T)$ persists.³¹

A correlation between nesting and possible Van Hove logarithmic singularities is demonstrated by a two-dimensional tight-binding energy band. If only nearest neighbors are considered, the nesting condition³² is satisfied only when the Fermi energy is close to half filling; this case corresponds to μ near the Van Hove peak in the density of states. By contrast, the inclusion of next-nearest-neighbor terms in the Hamiltonian can generate a variety of topologies that exhibit nesting even though μ is relatively far from the singularity.

The above theoretical background indicates that the strange Knight shift and static susceptibility phenomena found in cuprates are not necessarily related directly to nesting. Furthermore, as we show below, the peculiar de-

crease in χ at low temperatures is counter to the trend expected for a chemical potential situated close to a Van Hove singularity.

We have constructed the model density of states shown in Fig. 2 with the goal of explaining the decreasing susceptibility via a simple physical picture. If we consider the shape of the derivative of the Fermi function as a function of energy, shown as the dashed curve in Fig. 2, it is evident that a narrowing of this function at low temperatures will result in a preferential weighting of the lower density of states above the threshold E_0 . Thus the susceptibility decrease as T is lowered is associated with cases where μ is slightly above E_0 , but not too close to the logarithmic singularity.

We now proceed to calculate the susceptibility for this model and make quantitative comparisons to experimental data. The calculation of the susceptibility is described in Sec. II. We compare our results to experimental measurements of the magnetic susceptibility and the Knight shift in Secs. III and IV, respectively, and conclude in Sec. V.

II. SUSCEPTIBILITY

The general form of the spin susceptibility for a system of electrons with energy dispersion $E_{\mathbf{k}}$ is

$$\chi(\mathbf{q}, \omega) = \sum_{\mathbf{k}} \frac{f(E_{\mathbf{k}+\mathbf{q}}) - f(E_{\mathbf{k}})}{\omega - E_{\mathbf{k}+\mathbf{q}} + E_{\mathbf{k}}}, \quad (1)$$

where $f(E_{\mathbf{k}})$ is the Fermi function. In the static, long-wavelength limit this reduces to

$$\chi(T) = - \sum_{\mathbf{k}} \frac{\partial f}{\partial E_{\mathbf{k}}}. \quad (2)$$

The standard transformation to an energy variable introduces the density of states per spin defined by

$$N(E) = \sum_{\mathbf{k}} \delta(E - E_{\mathbf{k}}), \quad (3)$$

and thus leads to the final expression for the susceptibility

$$\chi(T) = \frac{1}{4\tau} \int_{-W_1}^{W_2} N(E) \operatorname{sech}^2 \left[\frac{E - \mu}{2\tau} \right] dE, \quad (4)$$

where $\tau = k_B T$ is the temperature and $W_1 + W_2$ is the full bandwidth.

The conventional Pauli susceptibility of ordinary metals refers to a form of $N(E)$ which is nearly independent of energy. In that case the integration over energy in Eq. (4) produces a constant susceptibility whose magnitude is proportional to the density of states at the Fermi energy $N(\mu)$.

We use the model density of states in Fig. 2 defined by the function

$$N(E) = \begin{cases} A + B \ln \left[\frac{E_0}{E_0 - E} \right], & E \leq E_0, \\ B \ln \left[\frac{E_0}{E - E_0} \right], & E > E_0, \end{cases} \quad (5a)$$

$$N(E) = \begin{cases} A + B \ln \left[\frac{E_0}{E_0 - E} \right], & E \leq E_0, \\ B \ln \left[\frac{E_0}{E - E_0} \right], & E > E_0, \end{cases} \quad (5b)$$

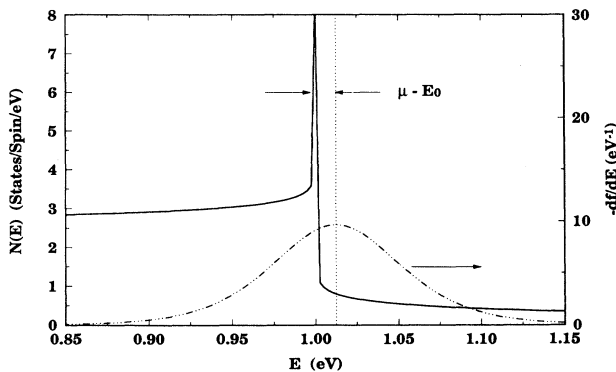


FIG. 2. Model density of states $N(E)$ used in the analysis is shown by the solid curve. The thermal broadening of the dashed curve $-df/dE$ (shown here at $T=300$ K), where f is the Fermi function, determines the region of the density of states that dominates the susceptibility and Knight shift. For $\mu_\mu > E_0$, lowering the temperature narrows the thermal broadening function and thus yields a decreasing $\chi(T)$ by virtue of the model step shape. By contrast, if μ_μ is right on or slightly below the logarithmic singularity at E_0 an upturn in χ at low T occurs.

where A, B are constants. The Van Hove singularity is located at the energy E_0 , which is also the threshold for the step function. For simplicity we choose $E_0 = 1$ eV throughout this study, and limit the range of the energy $0 < E \leq 2E_0$. We assume that the energy bandwidth is greater than 0.5 eV in order to have a cutoff much larger than the spread of the thermal function. The limits of integration in Eq. (4) can then be approximated by $\pm \infty$.

The evaluation of Eq. (4) for the step-function contribution to the density of states in Eq. (5a) gives

$$\chi_{\text{step}}(T) = \frac{A}{2} \left[1 + \tanh \left[\frac{E_0 - \mu}{2\tau} \right] \right]. \quad (6)$$

$$\chi_{\text{VH}} = B \left\{ \ln \left[\frac{E_0}{2\tau} \right] - \frac{1}{2} \int_0^\infty dx \ln(x) [\text{sech}^2(x - x_0) + \text{sech}^2(x + x_0)] \right\} \quad (7)$$

with $x = E/2\tau$ and $x_0 = (E_0 - \mu)/2\tau$. The dominant contribution to the temperature dependence of this term is seen in the limit $x_0 \rightarrow 0$. Physically, this corresponds to having the Fermi energy exactly at the Van Hove logarithmic singularity ($\mu = E_0$). The exact result in this limit is

$$\chi_{\text{VH}}(T, x_0 = 0) = B \ln \left[\frac{2E_0 e^\gamma}{\pi\tau} \right], \quad (8)$$

where $\gamma = 0.577$ is Euler's constant. Hence in this case the susceptibility increases logarithmically as the temperature T is lowered.

For the general case of $E_0 \neq \mu$ (or $x_0 \neq 0$) we evaluate

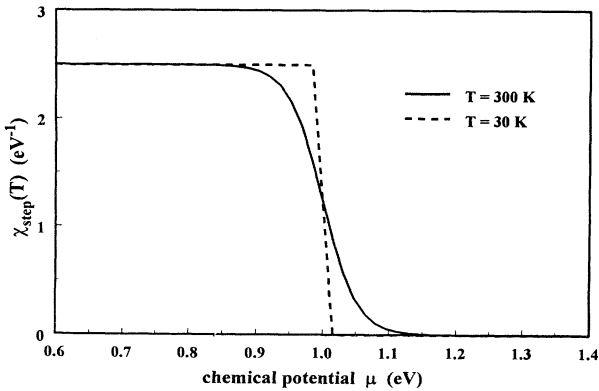


FIG. 3. The contribution to the susceptibility χ_{step} [Eq. (6)] from the step in the density of states is shown as a function of chemical potential μ at two temperatures, $T = 30$ and 300 K. The parameter $A = 2.5$ eV $^{-1}$ is the value used for fitting the LSCO value (see Table I). The anomalous decrease in χ as T is lowered occurs when $\mu > E_0 = 1$ eV. However, a surprising low T upturn in χ_{step} can happen in the narrow region $0.9 < \mu < 1.0$ eV even without the logarithmic singularity in the density of states.

This is shown in Fig. 3 at two different temperatures, 30 and 300 K. Note that this contribution to the susceptibility decreases as the temperature is lowered if the Fermi energy μ is somewhat above the threshold $E_0 = 1$ eV. Conversely, if the Fermi energy is slightly below E_0 , χ_{step} increases as T is lowered, as seen in Fig. 3 for the case that μ is held constant. The chemical potential will change as a function of temperature to preserve conservation of quasiparticle number. By itself, the step function generates an increase in μ with temperature, as we consider explicitly below.

The contribution of the Van Hove singularity to the susceptibility χ_{VH} can be expressed as

the integral χ_{VH} using contour integration. To do this, we expand the function $\text{sech}^2(x)$ in Eq. (7) using its power series expansion³⁵

$$\text{sech}^2(x) = 2 \sum_{n=0}^{\infty} \frac{(n + \frac{1}{2})^2 \pi^2 - x^2}{[(n + \frac{1}{2})^2 \pi^2 + x^2]^2}. \quad (9)$$

The resulting susceptibility is

$$\chi_{\text{VH}}(T) = B \left[\ln \left[\frac{E_0}{2\pi\tau} \right] - \text{Re}\Psi \left[\frac{1}{2} + \frac{i(E_0 - \mu)}{2\pi\tau} \right] \right], \quad (10)$$

where Ψ is the digamma function. The final result for the noninteracting electron susceptibility is then

$$\chi_0(T) = \chi_{\text{step}} + \chi_{\text{VH}}. \quad (11)$$

The principal mystery of a declining $\chi(T)$ at low temperatures can be traced to the step in the density of states. As seen from Fig. 3, this behavior will occur only when the Fermi energy μ is slightly above E_0 , because the narrowing of the thermal function with decreasing temperature (see Fig. 2) reduces the influence of the high density of states region below E_0 . However, if μ is sufficiently close to E_0 , this reduced sampling of the step below E_0 is partially offset by the contribution of the logarithmic peak. When the Fermi energy μ is located exactly at E_0 , the density of states peak is responsible for the logarithmic divergence in χ_{VH} [Eq. (8)] as $T \rightarrow 0$. The term containing the digamma function [Eq. (10)] is only weakly temperature dependent, as we confirm by numerical integration of Eq. (7) as well as the evaluation of the digamma function.

The logarithmic peak in the density of states also plays an important role in stabilizing the temperature variation of the chemical potential μ . This has a weak temperature dependence owing to the requirement that the total number of states at a given doping concentration, N_T , given by

$$N_T = \int_{-W_1}^{W_2} N(E) f(E, \mu, T) dE \quad (12)$$

remains constant. In the analysis presented in the next section, we use our model susceptibility to fit experimental data for the LSCO, BSCCO, and YBCO cuprates. The fits are generated by fixing the constants A and B for a given cuprate family, and varying only the zero-temperature value of the chemical potential μ_0 . We include in our model calculations the temperature-dependent chemical potential $\mu(T)$ determined self-consistently from the above constraint of Eq. (12). Typical shifts in $\mu(T)$ are of order $k_B T$ as expected.

We also test the effect of Coulomb interactions in the cuprates through a Stoner enhancement factor in the susceptibility,

$$\chi(T) = \frac{\chi_0(T)}{1 - U\chi_0(T)}, \quad (13)$$

where U is the interaction strength. In our analysis of the cuprates, we only consider weak interactions, and examine cases with $U \leq 0.5$ eV. This range of U values avoids the magnetic phase instability whose boundary is determined by the point where the susceptibility in Eq. (13) diverges. Hence the experimentally measured values of the static susceptibility provide constraints on the allowed values of U which are consistently less than the energy bandwidths in the range 1–2 eV determined by photoemission data.

III. CUPRATE SUSCEPTIBILITY

The principal features of the susceptibility anomalies considered here were originally found in the LSCO cuprate by Johnston *et al.*² and reviewed in comparison to other cuprates.¹ Our analysis of the LSCO data of Torrance *et al.*³ is shown in Fig. 4. The theory curves calculated using Eqs. (6) and (10) are generated by fixing the constants A , B , and U at the values given in Table I, and changing only the zero-temperature starting value μ_0 of the chemical potential. The upturn in $\chi(T)$ at low T indicates the influence of the logarithmic singularity in the density of states when μ_0 is very close to the threshold E_0 . The calculated dot-dashed curve fits the data triangles corresponding to a Sr content of $x = 0.25$. However, the data on samples with higher superconducting transition temperatures in this cuprate family (solid circles and

TABLE I. Parameters used to fit the susceptibility data. In all cases the Van Hove peak and the threshold in the density of states are located at $E_0 = 1$ eV. We use the conversion factor $0.645 \text{ eV} \times 10^{-4} \text{ emu/mol}$ to compare our calculated susceptibility to experiments.

Cuprate	A (eV ⁻¹)	B (eV ⁻¹)	$\mu_0 - E_0$ (eV)	U (eV)
La _{1.85} Sr _{0.15} CuO ₄	2.5	0.18	0.0199	0.32
La _{1.75} Sr _{0.25} CuO ₄	2.5	0.18	0.0023	0.32
Bi ₂ Sr ₂ CaCu ₂ O ₈	3.7	0.16	0.025	0.32
YBa ₂ Cu ₃ O ₇	1.28	0.195	-0.20	0
YBa ₂ Cu ₃ O _{6.63}	1.28	0.195	0.031	0.5

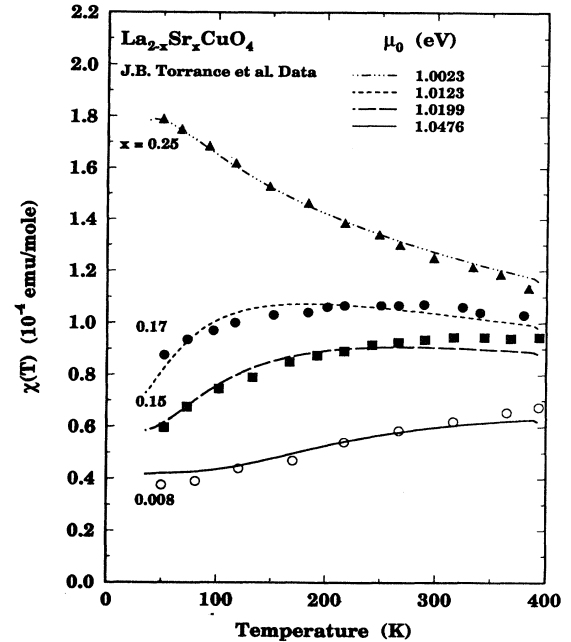


FIG. 4. Comparison of the calculated model susceptibility to the experimental data of Torrance *et al.* (Ref. 3) on LSCO. Fits to the susceptibility $\chi(T)$ for four different Sr dopings were produced by only varying μ_0 , the chemical potential at $T=0$. The values of μ_0 used for each theoretical curve are shown in the upper right hand corner. All other parameters are held constant at the values shown in Table I.

squares) exhibit a surprising downtrend in the susceptibility at low T . The latter cases are fit by the long-dashed curve (for $x=0.15$), and the short-dashed curve (for $x=0.17$) which require μ_0 to be further above the threshold E_0 than the case of highest Sr doping, $x=0.25$.

A correlation of the superconducting transition temperature with the model density of states $N(x)$ follows on the assumption that the Sr doping in LSCO merely shifts the Fermi energy in a rigid-band model. Assuming a linear dependence of the Fermi energy on x , the measured T_c values^{3,36} are shown in comparison to the extrapolated $N(x)$ values in Fig. 5. This plot indicates that a high density of states occurs for some low- T_c alloys (e.g., $x=0.25$) and some alloys with high values of T_c correspond to low regions of $N(x)$ (as in the case of $x=0.15$). It is intriguing that the maximum T_c cases cluster away from the threshold in $N(x)$ which also pinpoints the logarithmic peak. Remarkably, the two lowest T_c LSCO samples appear to be situated the closest to the Van Hove singularity.

IV. KNIGHT SHIFT

Nuclear magnetic resonance (NMR and NQR) techniques provide a unique microscopic probe of the spin response at specific atoms and sites in a compound. Extensive measurements⁴ on the YBCO cuprate reveal a Knight shift $K(T)$ emanating from the Cu-O planes that

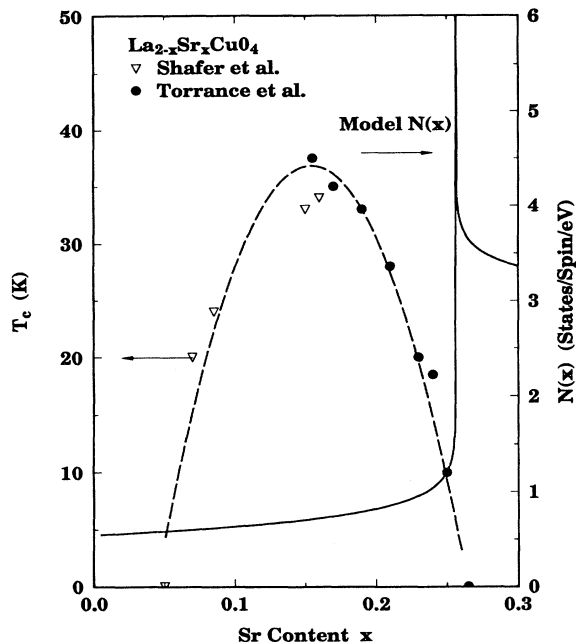


FIG. 5. Correlation of the model density of states at the Fermi energy (solid curve) with the superconducting transition temperature T_c (left scale) as a function of Sr content x . The model fits to the susceptibility were combined with a presumed linear dependence of μ_0 on x to estimate $N(x)$ (right scale). The dashed curve is sketched through the data points (taken from Refs. 3 and 36) as a guide to the eye.

exhibits similar temperature variations for the copper and oxygen sites, which indicates that an itinerant electron susceptibility is evident in the superconducting phases of this cuprate.

Careful scrutiny⁴ of the hyperfine coupling to the nuclear spins indicates that an appropriate representation for the Knight shift is

$$K(T) = \alpha\chi(T) + K_{\text{orb}}, \quad (14)$$

where α is a hyperfine coupling constant, and $\chi(T)$ is the planar spin susceptibility which we investigate here. In our analysis of the YBCO data, we assume that K_{orb} , the orbital contribution to the Knight shift, is zero. We determine the hyperfine coupling $\alpha = 0.57$ by comparing our computed susceptibility to the $\text{YBa}_2\text{Cu}_3\text{O}_7$ Knight shift data of Barrett *et al.*⁵ We then use this value to fit our computed curve to the Cu(2) Knight shift data of Takigawa *et al.*⁴ on $\text{YBa}_2\text{Cu}_3\text{O}_{6.63}$. Our coupling is qualitatively similar to the estimates used by Takigawa *et al.*⁴ which are influenced by their choice of a finite K_{orb} . The Stoner enhancement factor in Eq. (13) tends to amplify the temperature variation of $\chi(T)$ relative to $\chi_0(T)$. The values of U employed for the different materials are listed in Table I. In the case of the constant $\chi(T)$ in $\text{YBa}_2\text{Cu}_3\text{O}_7$, a finite U simply shifts the magnitude of the susceptibility, which could alternatively be achieved using a finite K_{orb} . Nevertheless, screening of the Coulomb

interaction by charge carriers may lead to a variation in U with oxygen content in YBCO as well as the other cuprates.

The $\text{YBa}_2\text{Cu}_3\text{O}_7$ Knight shift data of Barrett *et al.*⁵ in Fig. 6 reveals a standard Pauli susceptibility that is essentially temperature independent down to the superconducting transition at $T_c = 90$ K. This case suggests that the Fermi energy is relatively far from a Van Hove singularity of the logarithmic or step variety. We demonstrate a fit to the normal state component of this data by the solid curve. The principal ‘‘pseudogap’’ anomaly is seen in the data of Takigawa *et al.*⁴ for the oxygen depleted sample $\text{YBa}_2\text{Cu}_3\text{O}_{6.63}$ also shown in Fig. 6. Our calculated dashed curve fits the anomalous decrease in $\chi(T)$ at low temperatures quite well with a Fermi energy that is slightly above the step threshold energy E_0 . The logarithmic singularity is not the dominant feature for the YBCO cases shown here, but is included to retain the same model for all of the cuprates analyzed here. Also, the logarithmic peak tends to stabilize the shift in the chemical potential as a function of T .

Alloul *et al.*³⁷ have discovered a systematic evolution of the Knight shift as a function of oxygen content in YBCO, which suggests the general trend in the density of states shown in Fig. 7 if the Fermi energy is linearly related to the oxygen content. As oxygen is depleted, the

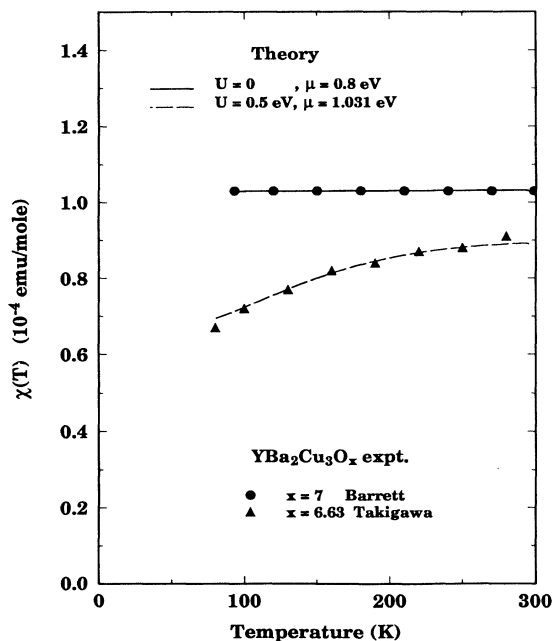


FIG. 6. The susceptibility data obtained from the Knight-shift measurements on $\text{YBa}_2\text{Cu}_3\text{O}_{7-\delta}$ reported in Refs. 4 and 5 are shown by circles and triangles. The solid curve is calculated with $\mu_0 - E_0 = -0.20$ eV which yields the standard Pauli behavior seen in the $\delta = 0$ data. The anomalous decrease in the $\delta = 0.37$ susceptibility data at low T is fit by the dashed curve which corresponds to a Fermi energy slightly above the step threshold in the model density of states. The parameters for YBCO are listed in Table I.

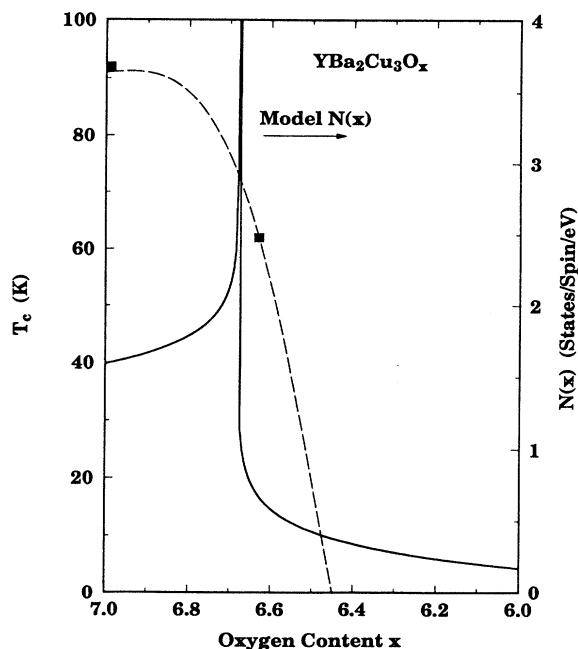


FIG. 7. The model density of states $N(x)$ at the Fermi energy is plotted as a solid curve using a linear variation of the Fermi energy shift as a function of oxygen content. The measured YBCO superconducting transition temperature T_c decreases with oxygen content (data squares), whereas the extrapolated $N(x)$ drops more dramatically. The dashed curve is a sketch of the well known trend of T_c as a function of doping in this cuprate.

present interpretation of their measured susceptibility indicates a shift of μ toward the step in $N(\mu)$. If the logarithmic singularity is indeed present in the region covered by these metallic compositions of YBCO alloys it should be possible to measure an upturn in χ at low T at a very specific composition. There is evidence⁸ for a susceptibility upturn in Zn-doped YBCO which has been interpreted previously as a localized magnetic moment contribution.

The above results are in contrast to the basic feature of the BCS theory of electron pairing that predicts a superconducting transition temperature that increases with the density of states. For the YBCO sample with $T_c = 60$ K, the low-temperature susceptibility suggests that the density of states is much lower than in the case of the $T_c = 90$ K compound. Similarly the LSCO density of states correlation with T_c shown in Fig. 5 is incompatible with the BCS weak-coupling formula for the transition temperature.

Finally we examine the Knight-shift data of Kitaoka⁶ and Takigawa⁷ on the Bi2212 superconductor which also displays the anomalous “pseudogap” drop at low T . In extracting the susceptibility from this data we leave in place the values of the hyperfine coupling α and K_{orb} employed by Kitaoka.⁶ Remarkably the same model that we have used above yields a good representation of the susceptibility as shown in Fig. 8 for a Fermi energy located

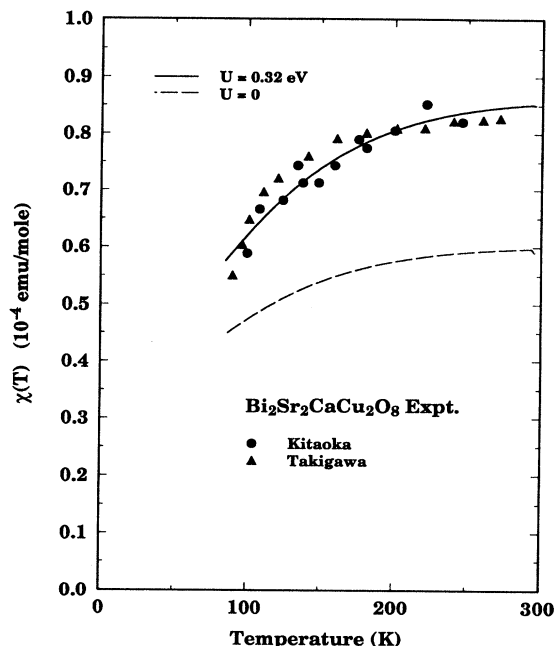


FIG. 8. The calculated susceptibility as a function of temperature is shown by the solid curve in comparison to the Bi2212 susceptibility estimated from the Knight shift data of Refs. 6 and 7. The anomalous decrease in χ at low T results from a Fermi energy slightly above the model step threshold. The model parameters for these cuprates are given in Table I. The dashed curve is the bare susceptibility with no Stoner enhancement.

above the threshold energy E_0 . The solid curve illustrates the effect of the Stoner enhancement in amplifying the temperature variation of $\chi(T)$ relative to the dashed curve for $\chi_0(T)$, plotted using $U=0$. Thus this high temperature superconductor with T_c above 80 K appears to correspond to a relatively low density of states.

Another case of a conventional Pauli susceptibility that is nearly constant is found in the thallium-based TBCO family of superconductors.⁶ However, it is very interesting that small changes in oxygen content create dramatic changes in the T_c values ranging from 85 down to 0 K, even though the corresponding measured susceptibility values are nearly identical and essentially independent of temperature.

V. CONCLUSIONS

A correlation of the superconducting transition temperatures of various cuprates with the model density of states is shown in Fig. 9. The T_c data points (circles, squares, and triangles) are plotted at the Fermi energy values used to fit the susceptibility data for each material. Although the corresponding magnitude of the density of states for these cuprates is uncertain, the placement of the Fermi energy relative to the threshold (i.e., $\mu - E_0$) provides insight into mechanisms that have been proposed for high-temperature superconductivity.

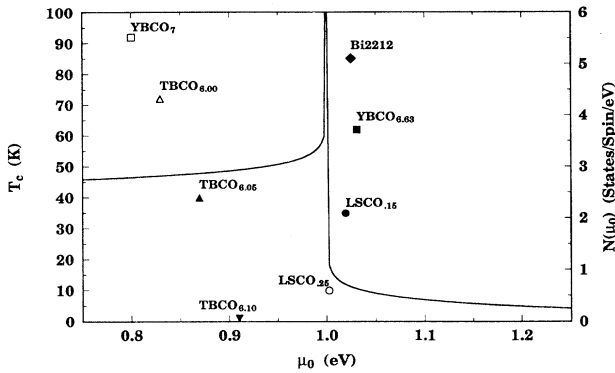


FIG. 9. Superconducting transition temperatures of several cuprates are shown at values of the Fermi energy obtained from our calculated fits to the susceptibility data. The general shape of the model density of states $N(E)$ is the same for all of the cuprates considered here, although the relative heights above and below the $N(E)$ threshold for a given material are in Table I. The solid curve is the density-of-states model with parameters appropriate to LSCO. Both $\text{YBa}_2\text{Cu}_3\text{O}_7$ and $\text{Tl}_2\text{Ba}_2\text{CuO}_{6+\delta}$ exhibit a constant susceptibility which only requires that the Fermi energy be in a region of constant $N(E)$. For our model, a Fermi energy $\mu_0 \leq 0.9$ eV will produce a constant $\chi(T)$.

The evidence for a large density of states just below the Fermi energy is further confirmed by recent photoemission data^{12–17} on several cuprates. This type of structure may naturally arise from a reasonably flat band whose maximum is very close to the Fermi energy. In the event that another broader band crosses the Fermi energy simultaneously, the narrow band may generate excitons³⁸ or perhaps acoustic plasmon modes³⁹ which may enhance pairing of electrons. The two-dimensional character of the cuprate electronic structure is particularly beneficial for reducing the Landau damping of the acoustic plasmons and therefore enhances their prospects for existing as well-defined excitations.⁴⁰ Photoemission spectroscopy reveals the existence of a nearly half-filled band in addition to a narrower band close to the Fermi band in YBCO (Ref. 13) and also in BSCCO.¹²

Conventional weak-coupling formulas for T_c within the BCS theory are clearly not compatible with the density of states trends shown in Fig. 9. However, several theoretical developments^{21–25} have emphasized the role of a logarithmic singularity in the density of states in enhancing the pairing caused by phonon exchange. Thus the very narrow region of the singularity shown in Fig. 9 and the correlation with T_c values of cuprates may provide constructive guidelines for quantitative calculations based on Van Hove singularities.

Our analysis predicts an upturn in the susceptibility as the temperature is lowered when the Fermi energy is right on the peak of the Van Hove logarithmic singularity. Thus the recent evidence for this desired placement of μ from photoemission by King *et al.*⁶ on a slightly doped Bi2201 cuprate presents a case where a future susceptibility measurement may test the validity of our analysis or the existence of the narrow logarithmic structure.

Another model using an inverse square-root singularity in the density of states has been investigated by Aristov and Yashenkin.⁴¹ Their model calculation also produces a temperature-dependent susceptibility which is reminiscent of the cuprate data.

Finally we note that the primary “pseudogap” anomaly of a decreasing susceptibility at low temperatures occurs in our analysis because of the threshold step function in our density of states model, and does not require the logarithmic singularity. The few cases in cuprates where the susceptibility rises at low temperatures are reminiscent of the *A-15* superconductors, where the anomalous rise may be attributed¹⁹ to a narrow peak in $N(E)$, with the logarithmic divergence providing one such example.

A possible physical origin of the band model that we have chosen may be traced to band-structure calculations¹⁰ such as the YBCO study by Mazin *et al.*¹¹ Another more esoteric explanation is the “spin bag” picture proposed by Kampf and Schrieffer.⁴² However, the latter perturbation theory treatment of antiferromagnetic spin fluctuations has not yet produced a specific “pseudogap” model for direct comparison. The Monte Carlo calculations suggest another source of band narrowing via many-body correlations.^{27,29}

Empirical band-structure models^{40,43} based on an anisotropic two-dimensional tight-binding approximation will produce the type of density-of-states model that is used in the present analysis. With the aid of experimental photoemission data, such band models may aid the investigation of other anomalous properties of the cuprates including the role of nesting and/or Van Hove peaks in spin-mediated mechanisms of superconductivity.⁴³

ACKNOWLEDGMENTS

It is a pleasure to acknowledge stimulating discussions with D. S. Dessau, Y. Ishii, D. C. Johnston, W. A. Little, J. V. Noble, and M. Takigawa. We appreciate NMR data sent to us by Y. Kitaoka and M. Takigawa. Two of us (J.R. and C.T.R.) appreciate the hospitality of Stanford University during a sabbatical visit under the auspices of the University of Virginia. Research at the University of Virginia was supported by DOE Grant No. DE-FG05-84ER45113.

¹See review by D. C. Johnston, *J. Magn. Mater.* **100**, 218 (1991).

²D. C. Johnston *et al.*, *Physica C* **153-155**, 572 (1988); *Phys. Rev. Lett.* **62**, 957 (1989).

³J. B. Torrance *et al.*, *Phys. Rev. B* **40**, 8872 (1989).

⁴M. Takigawa *et al.*, *Phys. Rev. B* **43**, 247 (1991), and references cited therein.

⁵The Cu(2) Knight shift data for $\text{YBa}_2\text{Cu}_3\text{O}_7$ is from S. E. Bar-

- rett *et al.*, Phys. Rev. B **41**, 6283 (1990).
- ⁶Y. Kitaoka *et al.*, J. Phys. Chem. Solids **54**, 1385 (1993), and references therein.
- ⁷M. Takigawa and D. B. Mitzi, J. Low Temp. Phys. **95**, 89 (1994).
- ⁸A. V. Mahajan, H. Alloul, G. Collin, and J. F. Marucco, Phys. Rev. Lett. **72**, 3100 (1994).
- ⁹J. Friedel, J. Phys. Condens. Matter **1**, 7757 (1989).
- ¹⁰W. E. Pickett, Rev. Mod. Phys. **61**, 433 (1989), and references cited therein.
- ¹¹I. I. Mazin *et al.*, Phys. Rev. B **46**, 11 232 (1992).
- ¹²D. S. Dessau *et al.*, Phys. Rev. Lett. **71**, 2781 (1993).
- ¹³K. Gofron *et al.*, J. Phys. Chem. Solids **54**, 1193 (1993).
- ¹⁴A. A. Abrikosov, J. C. Campuzano, and K. Gofron, Physica C **214**, 73 (1993).
- ¹⁵M. Onellion *et al.* (private communication).
- ¹⁶D. M. King *et al.*, Phys. Rev. Lett. **73**, 3298 (1994).
- ¹⁷K. Gofron *et al.*, Phys. Rev. Lett. **73**, 3302 (1994), and references cited therein.
- ¹⁸M. Weger and I. B. Goldberg, in *Solid State Physics*, edited by H. Ehrenreich, F. Seitz, and D. Turnbull (Academic, London, 1973), Vol. 28, p. 1.
- ¹⁹A. M. Clogston and V. Jaccarino, Phys. Rev. **121**, 1357 (1961).
- ²⁰J. Labbé and J. Friedel, J. Phys. (Paris) **27**, 153 (1966).
- ²¹J. E. Hirsch and D. J. Scalapino, Phys. Rev. Lett. **56**, 2732 (1986).
- ²²I. E. Dzyaloshinski, Zh. Eksp. Teor. Fiz. **93**, 1487 (1987) [Sov. Phys. JETP **66**, 848 (1987)].
- ²³P. A. Lee and N. Read, Phys. Rev. Lett. **58**, 2692 (1987).
- ²⁴D. M. Newns, P. C. Pattnaik, and C. C. Tsuei, Phys. Rev. B **43**, 3075 (1991).
- ²⁵R. S. Markiewicz, Physica C **217**, 381 (1993), and references therein.
- ²⁶R. J. Radtke, K. Levin, H. B. Shuttler, and M. R. Norman, Phys. Rev. B **48**, 15 957 (1993).
- ²⁷E. Dagotto, A. Nazarenko, and M. Boninsegni, Phys. Rev. Lett. **73**, 728 (1994).
- ²⁸See, for example, T. Barnes, Int. J. Mod. Phys. C **2**, 659 (1991), and references cited therein.
- ²⁹E. Dagotto, Rev. Mod. Phys. **66**, 763 (1994).
- ³⁰H. Takagi *et al.*, Phys. Rev. Lett. **69**, 2975 (1992). A crossover from linear T resistivity to a T^2 variation occurs in $Tl_2Ba_2CuO_{6+\delta}$ as a function of oxygen content as found by Y. Kubo, Phys. Rev. B **43**, 7875 (1991).
- ³¹A. Virosztek and J. Ruvalds, Phys. Rev. B **42**, 4064 (1990).
- ³²J. Ruvalds, C. T. Rieck, J. Zhang, and A. Virosztek, Science **256**, 1664 (1992).
- ³³J. Rossat-Mignod *et al.*, Physica B **169**, 58 (1991); Physica C **185-189**, 86 (1991).
- ³⁴R. J. Birgeneau *et al.*, Z. Phys. B **87**, 15 (1992).
- ³⁵I. S. Gradshteyn and I. M. Ryzhik, *Tables of Integrals, Series, and Products* (Academic, New York, 1980), p. 36.
- ³⁶M. W. Shafer, T. Penney, and B. L. Olsen, Phys. Rev. B **36**, 4047 (1987).
- ³⁷H. Alloul, P. Mendels, G. Collin, and P. Monod, Phys. Rev. Lett. **61**, 746 (1988).
- ³⁸W. A. Little, Phys. Rev. **134**, A1416 (1964).
- ³⁹J. Ruvalds, Adv. Phys. **30**, 677 (1981), and references cited therein.
- ⁴⁰J. Ruvalds, Phys. Rev. B **35**, 8869 (1987); Y. Ishii and J. Ruvalds, *ibid.* **48**, 3455 (1993).
- ⁴¹D. N. Aristov and A. G. Yashenkin, Physica C (to be published).
- ⁴²A. Kampf and J. R. Schrieffer, Phys. Rev. B **41**, 6399 (1990).
- ⁴³J. Ruvalds, C. T. Rieck, S. Tewari, J. Thoma, and A. Virosztek, Phys. Rev. B **51**, 3797 (1995).